Insect Molecular Biology

Insect Molecular Biology (2013) doi: 10.1111/imb.12035

Noncanonical expression of *caudal* during early embryogenesis in the pea aphid *Acyrthosiphon pisum*: maternal *cad*-driven posterior development is not conserved

C-c. Chang[1]*†‡, Y-m. Hsiao[1]*††, T-Y. Huang*§, C. E. Cook¶, S. Shigenobu and T-H. Chang‡††**

**Laboratory for Genetics and Development, Department of Entomology/Institute of Biotechnology, College of Bio-Resources and Agriculture, National Taiwan University, Taipei, Taiwan; †Research Center for Developmental Biology and Regenerative Medicine, National Taiwan University, Taipei, Taiwan; ‡Genome and Systems Biology Degree Program, National Taiwan University, Taipei, Taiwan; §Institute of Biochemical Sciences, College of Life Science, National Taiwan University, Taipei, Taiwan; ¶EMBL-European Bioinformatics Institute, Wellcome Trust Genome Campus, Hinxton, UK; **NIBB Core Research Facilities, National Institute for Basic Biology, Okazaki, Japan; ††Genomics Research Center, Academia Sinica, Taipei, Taiwan*

Abstract

Previously we identified anterior localization of *hunchback* (*Aphb*) mRNA in oocytes and early embryos of the parthenogenetic and viviparous pea aphid *Acyrthosiphon pisum*, suggesting that the breaking of anterior asymmetry in the oocytes leads to the formation of the anterior axis in embryos. In order to study posterior development in the asexual pea aphid, we cloned and analysed the developmental expression of *caudal* (*Apcad*), a posterior gene highly conserved in many animal phyla. We found that transcripts of *Apcad* were not detected in germaria, oocytes and embryos prior to the formation of the blastoderm in the asexual (viviparous) pea aphid. This unusual expression pattern differs from that of the existing insect models, including long- and short-germ insects, where maternal *cad* mRNA is passed to the early embryos and forms a posterior–anterior gradient. The first detectable *Apcad* expression occurred in the newly formed primordial germ cells and their adjacent blastodermal cells during late blastulation. From gastrulation onward, and as in other insects, *Apcad* mRNA is restricted to the posteriormost region of the germ band. Similarly, in the sexual (oviparous) oocytes we were able to identify anterior localization of *Aphb* mRNA but posterior localization of *Apcad* was not detected. This suggests that *cad*-driven posterior development is not conserved during early embryogenesis in asexual and sexual pea aphids.

Keywords: *caudal*, posterior axis, parthenogenetic viviparous, asymmetric localization, *hunchback*.

Correspondence: Chun-che Chang, Laboratory for Genetics and Development, Department of Entomology, National Taiwan University, no. 27, Lane 113, Roosevelt Road, Sec. 4, Taipei 106, Taiwan. Tel.: +8862 33665578; fax: +8862 27369366; e-mail: chunche@ntu.edu.tw

[1]Equal contribution.

Introduction

Establishment of the body axes is crucial to pattern formation in animals. In model organisms such as *Drosophila melanogaster* (fly; Lall & Patel, 2001), *Danio rerio* (zebrafish; Langdon & Mullins, 2011), and *Xenopus laevis* (frog; Weaver & Kimelman, 2004), body axes are preformed in the oocytes via asymmetric localization of maternal factors; this key process is required to break the egg symmetry before fertilization. The nematode *Caenorhabditis elegans* adopts similar mechanisms to specify the body axes but asymmetric partitioning of maternal factors such as Par proteins in the single cell eggs, is induced by fertilization (Pellettieri & Seydoux, 2002). In *Mus musculus* (mouse), however, a preformed body axis has not been identified in the oocytes and it is believed that axis determination is accomplished by serial specification of cell lineages under multiple cellular environments (Takaoka & Hamada, 2012).

Of all animal models, the molecular networks involved in axis formation are best understood for *Drosophila*. In *Drosophila*, establishment of both anterior–posterior (AP) and dorsal–ventral (DV) axes is initiated by the signalling of Gurken (Grk), a transforming growth factor α-like epidermal growth factor ligand, from oocytes to follicle cells in the posterior and dorsal regions, respectively. During mid-oogenesis, the nucleus positioned at the posterior cortex of the oocyte triggers Grk signalling into the follicle cells. Afterwards, signals delivered back to the oocyte reorganize the polarization of the cytoskeleton (Gonzalez-Reyes *et al*., 1995), facilitating the asymmetric localization of *bicoid* (*bcd*) mRNA to the anterior and *oskar* (*osk*) mRNA to the posterior for establishing the AP axis. The nucleus then migrates toward the anterior dorsal region, secreting *grk* mRNA to break the DV symmetry and then drive a molecular cascade to establish DV polarity (Kugler & Lasko, 2009).

Nevertheless, it is clear that *bcd*, an anterior determinant in *Drosophila*, is a recent invention of dipterans and posterior localization of *osk* mRNA can only be identified in holometabolous insects (Stauber *et al*., 2002; Lynch & Desplan, 2003; Extavour, 2011; Lynch *et al*., 2011). In *Gryllus bimaculatus* (cricket), a hemimetabolus insect model, expression of *osk* was recently identified in neuroblasts of the brain and central nervous system; however, *osk* was neither posteriorly localized in the oocytes nor specifically expressed in germ cells (Ewen-Campen *et al*., 2012). This implies that asymmetrically localized molecules for establishing the AP axis may vary within insect species. For example, in the wasp *Nasonia vitripennis* (Hymenoptera) breaking of asymmetry is evidenced by the posterior localization of *osk* (Lynch *et al*., 2011), *nanos* (*nos*) and *caudal* (*cad*) mRNAs (Olesnicky & Desplan, 2007). Maternal *orthodenticle* (*otd*) mRNA is localized to the anterior as well as the posterior poles of late oocytes and early embryos prior to blastoderm formation. Functional analyses show that: (1) the synergistic interaction between *otd* and *hunchback* (*hb*) specifies anterior development (Lynch *et al*., 2006); and (2) *osk*, *nos* and *cad* are involved in germline specification and posterior determination (Olesnicky *et al*., 2006; Lynch & Desplan, 2010; Lynch *et al*., 2011).

In contrast to the long-germ insects such as *Drosophila* and *Nasonia*, where all body segments are specified almost simultaneously by gastrulation, how the AP axis of the embryo relates to the AP polarity of the egg is much less understood in short-germ insects such as the beetle *Tribolium castaneum* (Coleoptera), where the formation of posterior segments requires a secondary phase of growth in the abdomen (Schröder *et al*., 2008). In *Tribolium*, serious defects of development in the head, thorax and anterior abdomen were identified in larvae subjected to parental RNA interference (RNAi) against both *hb* and *otd* (Schröder, 2003). This suggests that synergistic interaction between *hb* and *otd* specifies anterior development in *Tribolium* as *bcd* does in *Drosophila*, although anterior localization of *hb* and *otd* mRNA in oocytes and early eggs was not detected (Wolff *et al*., 1995; Schröder, 2003). Recent studies show that *axin* mRNA, which encodes a negative regulator of the Wnt signalling pathway, is localized to the anterior pole of the newly laid eggs and knockdown of *axin* causes anterior defects in progeny (Fu *et al*., 2012); however, whether there exists a posterior determinant in the egg remains uncertain. Although parental RNAi of *nos*, a conserved posterior determinant in insects, can cause defects in abdominal segmentation, how *nos* is patterned in eggs and early embryos requires further clarification in *Tribolium* (Schmitt-Engel *et al*., 2012). Similarly, although accumulation of *nos* mRNA and Nos protein is identified in the posterior region of eggs and embryonic primordia in the grasshopper *Schistocerca americana* (Lall *et al*., 2003), a short-germ insect like *Tribolium*, functional analysis of *nos* is critical to the understanding of whether the establishment of egg polarity can affect the formation of the embryonic axis in the posterior area.

In the parthenogenetic and viviparous pea aphid *Acyrthosiphon pisum*, a hemimetabolous hemipteran without orthologues of *bcd* and *osk* (Shigenobu *et al*., 2010), we have identified anterior localization of *hb* (*Aphb*) mRNA in the oocytes and early embryos prior to gastrulation. This supports the existence of a preformed anterior axis in the asexual pea aphid (Huang *et al*., 2010). Posterior localization of Nos was not observed in the oocytes and its appearance was first detected later in egg chambers undergoing nuclear division – a developmental status designated as the onset of embryogenesis in the asexual ovarian tubules (ovarioles) (Chang *et al*., 2006). This is so far the earliest posterior polarity we can identify in the asexual pea aphid, suggesting that either we have not found a posterior molecule concurrently localized with the anterior *hb* mRNA or formation of the anterior polarity precedes that of the posterior polarity. In order to understand whether the posterior polarity is formed as early as the anterior polarity in the asexual pea aphid, we studied the developmental expression of *cad* because: (1) homologues of *cad* have been widely identified in animal phyla and their roles in posterior development are highly conserved (Copf *et al*., 2004; McGregor *et al*., 2009); (2) the anterior localization of *Aphb* implies that the asexual pea aphid may specify the AP axis by localizing transcripts of *Drosophila* homologues in directing anterior and posterior development (Huang *et al*., 2010), and *cad* is one of the posterior candidates; and (3) in *Nasonia* localization of *cad* mRNA is restricted to the oosome (germ plasm) in the posterior region of oocytes and early embryos (Olesnicky *et al*., 2006), suggesting that posterior localization of *cad* mRNA can be detected in some insects with a preformed

germ plasm in the egg posterior, and the asexual pea aphid, known to possess a posteriorly localized germ plasm (Chang *et al*., 2006), may be such a case.

In *Drosophila*, *cad* is transcribed both maternally and zygotically (Mlodzik *et al*., 1985). Maternal *cad* mRNA is first detected in the nurse cells during early oogenesis, and then is transported to the oocytes from mid-oogenesis onward. Even distribution of *cad* mRNA remains in oocytes and syncytia before cellularization. During the 13th nuclear division, *cad* mRNA is down-regulated in the anterior region and a posterior-to-anterior gradient of *cad* transcripts is displayed in syncytia undergoing cellularization. Soon after the beginning of gastrulation, the zygotic *cad* mRNA is restricted to a stripe 3–5 cells in width near the posterior pole of the egg chamber. During further development – from extension to retraction of the germ band – the *cad*-positive cells are located in the posteriormost region of the embryo, which will then differentiate into the hindgut and terminal structures of the abdomen (Mlodzik *et al*., 1985; Mlodzik & Gehring, 1987). The restriction of transcripts to the posterior end of the germ band has become a signature of *cad* genes in *Drosophila* as well as other insects mentioned above, regardless of long- or short-germ developmental modes (Copf *et al*., 2004). If pea aphids adopted this conserved feature of *cad*, we expected to label the posteriormost part of the newly cellularized germ band, which was neither morphologically prominent nor marked, using antisense riboprobes of posterior genes such as *Apnos* (Chang *et al*., 2009) in the asexual pea aphid.

Accordingly, in order to understand posterior determination and posterior development in the asexual pea aphid, we have cloned the aphid orthologue of the *cad* gene (*Apcad*) and detected its developmental expression using *in situ* hybridization. Through the analysis of *Apcad* expression, we found conserved and divergent roles of the *cad* gene that help enlighten how the aphid posterior is patterned in the asexual phase of reproduction. We also detected the co-expression of *Aphb* and *Apcad* in both asexual and sexual ovaries, with the aim of understanding how anterior (*Aphb*) and posterior (*Apcad*) genes are patterned in these two distinct types of eggs.

Results

Cloning and sequence analysis of the Apcad *gene*

Cloning and sequencing of *cad* homologues in the pea aphid was begun before the *A. pisum* genome sequence was available. We used a degenerate PCR approach to amplify sequences encoding the conserved homeodomain of Cad/Cdx (vertebrate Cad) proteins. These amplified a single PCR product, which we cloned and sequenced. Sequence alignment showed that 41 out of the 60 amino acids in the cloned sequence were identical to homeodomains of other Cad/Cdx proteins, with a similarity of amino acid residues of up to 80% (Fig. 1A). This suggests that our cloned sequence, designated as *Apcad*, is a *cad* homologue. Using rapid amplification of cDNA ends (RACE) PCR, we extended this sequence by an additional 271 base pairs (bp) outside the homeodomain. In total, we cloned and sequenced 451 bp of the *Apcad* gene (Fig. 1B) and this DNA fragment was used as a template for synthesizing an antisense riboprobe to detect the expression of *Apcad* mRNA.

Our degenerate PCR products contained only a single sequence, and there was no experimental indication of other *cad*-like sequences. After the aphid genome became available, we used nucleotide and protein BLAST to compare our cloned sequence to the aphid genome assembly (version 1, then version 2) both at the National Center for Bioinformation technology (NCBI; http://blast.ncbi.nlm.nih.gov/Blast.cgi) and on Ensembl Genomes (http://metazoa.ensembl.org/Acyrthosiphon_pisum/blastview). For both nucleotide and protein BLAST searches our cloned sequence matched, with 100% identity, a single locus in the aphid genome (NCBI Reference Sequence XM_003244354.1, NCBI reference protein XP_003244402.1, NCBI and AphidBase locus LOC100574453). This result is also consistent with that of Shigenobu *et al*. (2010), who reported only a single *cad*-like gene in version 1 of the aphid genome assembly. Our results thus strongly suggest that the pea aphid has a single copy of the *cad* gene. Our results also confirm experimentally that the gene models used to identify genes and splice junctions in the sequenced genome are, at least for this gene, accurate.

Developmental expression of Apcad *mRNA during early development*

The asexual pea aphid produces offspring parthenogenetically and viviparously. Accordingly, in each ovariole developing embryos are accommodated within the egg chambers in an assembly-line fashion (Blackman, 1978). As with telotrophic ovarioles in other insects, germaria containing trophocytes (nurse cells) are located to the anteriormost region of the ovariole in the asexual pea aphid and oocytes adjacent to the germaria are derived from the posterior trophocytes (Fig. 2A). Via maturation division of nuclei, oogenesis then enters into embryogenesis without the cost of fertilization (Miura *et al*., 2003). Surprisingly, in germaria, oocytes, and embryos prior to the cellularization of blastoderm we did not detect the expression of *Apcad* mRNA (Fig. 2A, B).

We first detected *Apcad* expression in the posterior region of the cellularized blastoderm. The *Apcad*-positive region, which was 2–3 cells in width, covered several posterior blastodermal cells, newly segregated primordial

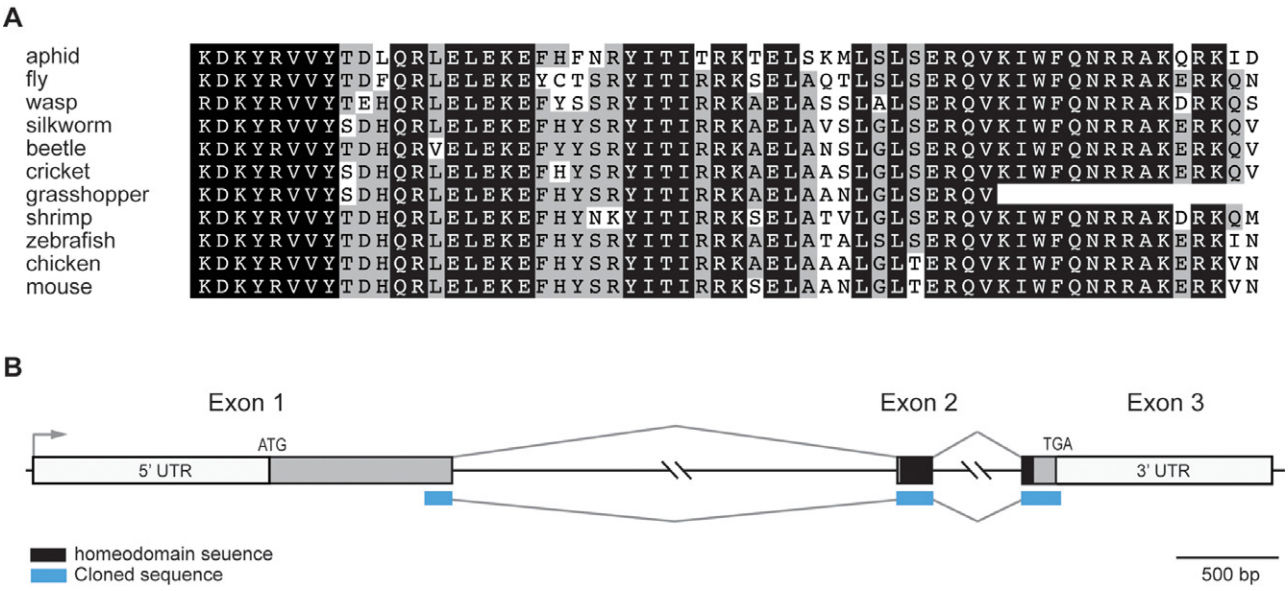

Figure 1. The *Apcad* gene. (A) Alignment of the homeodomain sequence of the ApCad protein against that of 10 other Caudal proteins across invertebrates and vertebrates. Identical amino acid sequences are boxed in black; grey boxes indicate sequence identity >50%. Fifteen amino acids in the C-terminus of the grasshopper Caudal homeodomain are not reported in the database. Species names and GenBank accession numbers of proteins are: aphid (*Acyrthosiphon pisum*, XP_003244402.1 (genome) and HF564623 (the present report)), fly (*Drosophila melanogaster*, NP_476954.1), wasp (*Nasonia vitripennis*, ABK39927.1), silkworm (*Bombyx mori*, NP_001037514.1), beetle (*Tribolium castaneum*, NP_001034498.1), cricket (*Gryllus bimaculatus*, BAD51739.1), grasshopper (*Schistocerca gregaria*, AAK56940.1), shrimp (*Artemia franciscana*, CAD98862.1), zebrafish (*Danio rerio*, NP_001092232.1), chicken (*Gallus gallus*, NP_990007.2), mouse (*Mus musculus*, NP_034010.3). (B) Genomic structure of *Apcad* as annotated in AphidBase (http://www.aphidbase.com/aphidbase/). Grey boxes, together with the black boxes that encode the homeodomain (HD), represent the coding regions. Clear boxes are the untranslated regions (UTRs). Blue boxes represent 451 base pairs (bp) of sequence from our PCR and 5′-rapid amplification of cDNA ends PCR experiments. Arrow: transcription initiation site; ATG: start codon; TGA: stop codon. Lengths (from 5′ to 3′): 5′ UTR, 982 bp; coding sequences, 1047 bp; 3′ UTR, 1057 bp. Scale bar, 500 bp.

germ cells (PGCs), and cells anteriorly adjacent to PGCs. Most of the *Apcad* transcripts were restricted to the PGCs (Fig. 2C). In addition, we used reverse transcription (RT)-PCR – a method more sensitive than *in situ* hybridization – to verify whether there was any residual expression of *Apcad* in early embryos. The RT-PCR results corresponded exactly to those carried out using *in situ* hybridization: expression of *Apcad* was not detected in germaria, oocytes and embryos prior to blastulation (Fig. 2D, E). This result shows that trophocytes in the germaria do not synthesize *Apcad* mRNA and that it is not passed to the oocytes and early embryos via the trophic cord.

Later, when all of the PGCs were aggregated near the centre of the egg chamber, expression of *Apcad* was elevated in one side of the posterior blastoderm (Fig. 2F, F′). When gastrulation began, *Apcad* expression was down-regulated in the PGCs (Fig. 2G). Moreover, we observed that strong signals of *Apcad* continued in the invaginating blastoderm flanking the blastopore (Fig. 2G, G′) – the initial opening for gastrulation and the entry of the endosymbiotic bacteria (endosymbionts) in the asexual pea aphid. However, the intensity of *Apcad* signals on the other side, which remained uninvaginated, was much weaker (Fig. 2G). In order to fully clarify whether preferential expression of *Apcad* occurs in the dorsal or ventral regions, molecular markers specific to cells in these two distinct areas are required but they are not yet available in the pea aphid. Nevertheless, as invagination of blastoderm occurs asynchronously in the asexual pea aphid and it is the dorsal blastoderm that first invaginates, later followed by the ventral blastoderm (Miura *et al.*, 2003), we infer that *Apcad* expression initially identified in the invaginating blastoderm is located on the dorsal side.

After the ventral blastoderm had folded inside the embryonic cavity, we could detect *Apcad* signals in the bilateral invaginating blastoderm with almost equivalent intensity (Fig. 2H). This indicates that the upsurge of the transcription level of *Apcad* in the dorsal and ventral invaginating blastoderm is not synchronous. Whether the increase of *Apcad* expression drives the invagination or whether *Apcad* expression is induced in the invaginating blastoderm remain open questions. Moreover, we found that both patches of the invaginating blastoderm became associated with each other, except in the region penetrated by the invading endosymbionts (Fig. 2H′). Expression of *Apcad* was not detected in germ cells after bilateral blastoderm invagination (Fig. 2H, H′).

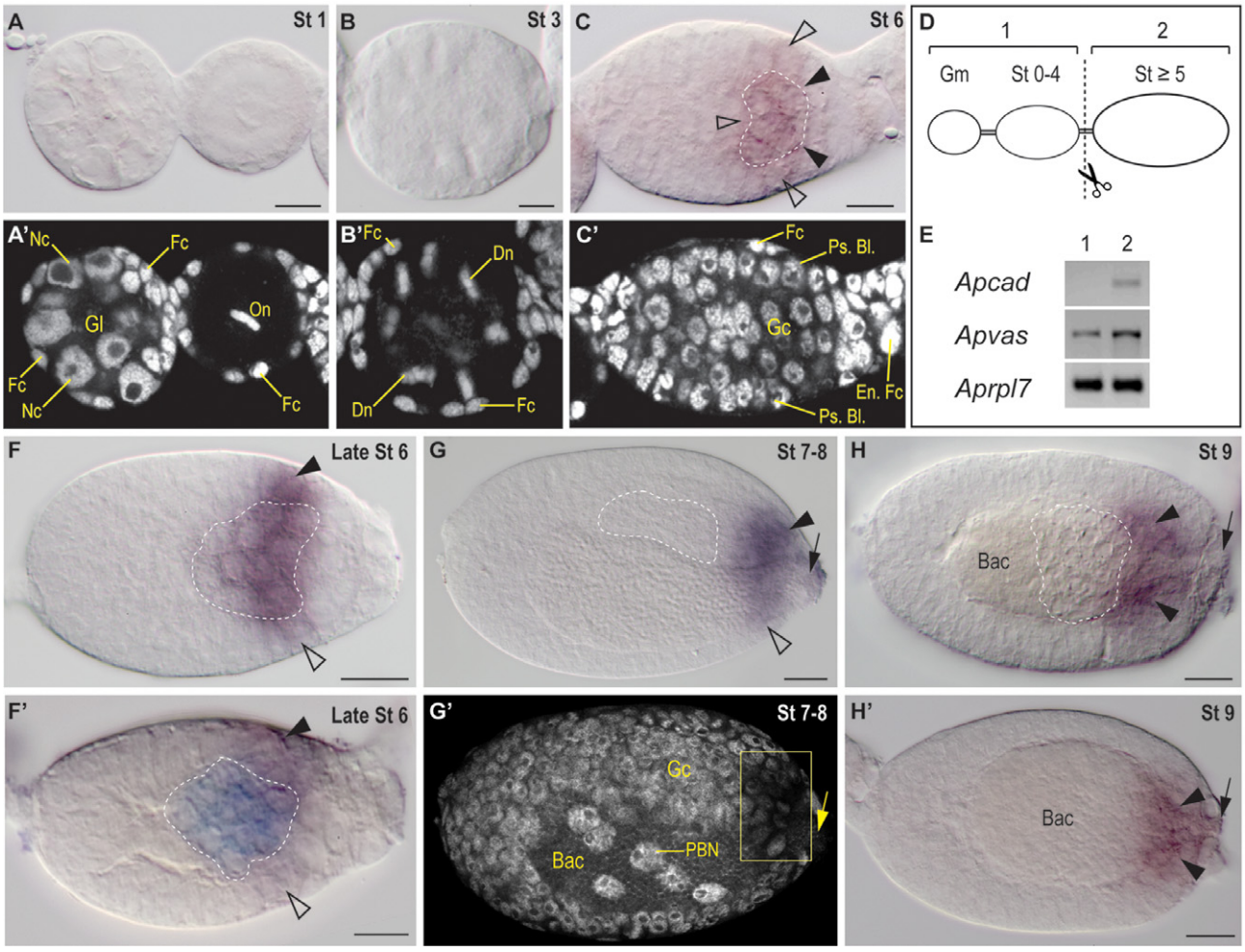

Figure 2. Developmental expression of *Apcad* mRNA during oogenesis and early embryogenesis. Unless otherwise noted, all embryos shown in this and other figures were produced asexually. (A)–(H) and (H′): single *in situ* of *Apcad*; (F′): double *in situ* of *Apcad* and *Apvas1*. Except (H′), where primordial germ cells (PGCs) are not shown in the focal plane, locations of PGCs are marked with dashed lines. Anterior region of egg chambers is to the left. Panels (A′)–(C′), and (G′) are nuclear staining of the preparations in (A)–(C) and (G), respectively. (A) Germaria and segregated oocytes (stage 1). (B) Embryos undergoing early syncytial synchronous nuclear divisions (stage 3). Expression of *Apcad* was not detected. (C) Embryos with newly formed PGCs (stage 6). Arrowheads indicate the expression of *Apcad* in germ cells with morphologically identifiable polar granules; hollow arrowheads designate weak expression of *Apcad* in cells that are adjacent to the segregated germ cells. (D, E) Comparison of *Apcad* expression between embryos before and after stage 4 of development. Group 1: germaria, oocytes and embryos at or before stage 4 of development; Group 2: embryos at or older than stage 5 of development. (D) outline of dissection. (E) Results of reverse transcription PCR. *Apcad* expression was not detected in Group 1 but it was detected in Group 2. *Apvas1*, positive control; *Aprpl7*, internal control. (F, F′) Embryos with segregated PGCs (late stage 6). *Apcad* expression became more prominent in one side of the posterior blastoderm (arrowhead) adjacent to the PGCs specifically labelled by the *Apvas1* riboprobe (blue, panel (F′)). Weak expression of *Apcad* was detected in blastodermal cells located at the opposite side (hollow arrowhead). In (F′), *Apcad* signals in PGCs could not be clearly distinguished because they were quenched by the colocalized *Apvas1* signals (blue). (G, G′) Incorporation of the maternal endosymbionts (stage 7) and early gastrulation (stage 8). Preferential expression of *Apcad* (arrowhead) was identified in the newly invaginating blastoderm located dorsally. Few transcripts of *Apcad* were detected in the ventral blastoderm that had not invaginated inward (hollow arrowhead). In (G′), yellow box marks *Apcad* expression in the dorsal invaginating blastoderm. (H, H′) Beginning of germ band invagination (stage 9). In (H), expression of *Apcad* mRNA with almost equivalent intensity was detected in blastoderm invaginating both dorsally and ventrally (arrowheads). Panel (H′) shows another stage-9 embryo taken at a different focal plane, displaying the closer proximity of the bilateral patches of invaginating germ band that expressed *Apcad* mRNA (arrowhead). Entry of endosymbionts is marked with arrows from panels (G) to (H′). Bac, bacteria; Dn, dividing nuclei; En. Fc, enlarged follicle cells; Fc, follicle cells; Gc, germ cells; Gl, germarial lumen; Gm, germaria; Nc, nurse cells; On, oocyte nucleus; Ps. Bl., posterior blastoderm; PBN, presumptive bacteriocyte nuclei; St, stages. Scale bar, 20 μm.

Developmental expression of Apcad *mRNA during mid- and late development*

In most insects, the differentiation of dorsal and ventral districts becomes prominent during gastrulation: the dorsal blastoderm becomes thinner and later further differentiates into the serosa; the ventral blastoderm becomes thickened and gives rise to the germ band. Like the early gastrula shown in Fig. 2H, the extending tips of both dorsal and ventral invaginating blastoderm, the germ

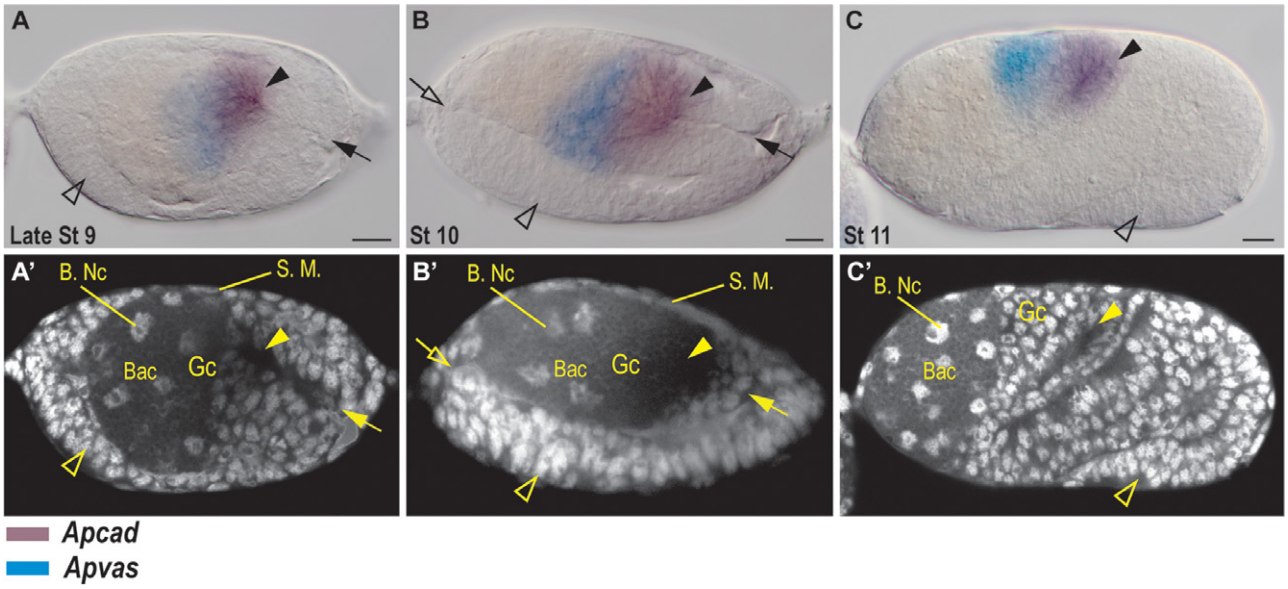

Figure 3. Developmental expression of *Apcad* mRNA during invagination and elongation of the germ band. Dissected ovarioles were hybridized with digoxigenin-labelled *Apcad* and fluorescein-labelled *Apvas1* antisense riboprobes concurrently. Colour keys indicating expression signals of *Apcad* and *Apvas1* are shown under the figure. Anterior region of egg chambers is to the left; dorsal is upper. Embryos in (A) and (B) are presented dorso-laterally; embryo in (C) is a lateral view. Panels (A′) to (C′) are nuclear stains of preparations shown in (A) to (C), respectively. Arrowheads, expression of *Apcad* mRNA; hollow arrowheads, locations of the cephalic lobes; arrows, furrows between invaginating germ band [not shown in the focal plane of (B′)]. (A, B) Invagination and bending of the germ band (stages 9 and 10). Expression of *Apcad* mRNA was restricted to the posteriormost region of the invaginating germ band. Embryo in (B) is slightly older than that in (A) because the invaginating germ band has reached to the middle region of the egg chamber. Discontinuity of the serosa and the presumptive cephalic lobe, a morphological feature of stage-10 embryos (B), is indicated with a hollow arrow. (C) Elongation of the germ band (S-shaped embryo, stage 11). In contrast to the embryos shown in (A) and (B), the cephalic lobe of the stage-11 embryos has migrated more posteriorly in the egg chamber and the elongating germ band folds into an S shape. Expression of *Apcad* remains at the posterior tip of the germ band. Abbreviations: Bac, bacteria; B. Nc, nuclei of the bacteriocytes; Gc, germ cells; S. M., serosal membrane; St, stage. Scale bar, 20 μm.

band in mid- and late gastrula embryos designated by Miura *et al*. (2003), expressed *Apcad* (Fig. 3A, B). Later, when the germ band extended as an S-shaped embryo (an embryonic structure that is formed by the invagination of the germ band and the inversion of the AP axis), we identified *Apcad* transcripts restricted to the posteriormost region (Fig. 3C). Because no furrows were visible within the *Apcad*-positive region of S-shaped embryos, we infer that it was fused by the dorsal and ventral tips of the invaginating germ band expressing *Apcad* (Fig. 3A, B) or even earlier during early gastrulation (Fig. 2H′). Our inference is supported by Will (1888) and Hagan (1951), where the realization of the 'closed blastopore' evidenced the fusion of dorsal and ventral tips of the invaginating germ band (Will, 1888; Hagan, 1951).

While the germ band continued to extend, *Apcad* expression persisted in the posterior terminal region of the abdomen (Fig. 4A–D). We observed that the ratio of *Apcad*-positive area to the posterior abdomen became reduced after katatrepsis [embryo flip (Fig. 4C)]. This might be caused by the expansion of the abdominal termini or by the reduction of *Apcad*-positive cell numbers. In mature embryos after germ band retraction, we identified *Apcad* transcripts restricted to the final segment of the abdomen (Fig. 4D, E) and the posterior proctodeum [hindgut (Fig. 4F)].

Comparison of Aphb *and* Apcad *expressions in asexual and sexual ovarioles*

We extended the detection of *Apcad* expression in the sexual (oviparous) ovarioles to understand how maternal *Apcad*, if there was any, was patterned in the oocytes. Meanwhile, we examined the expression of *hb* (*Aphb*) using double *in situ* hybridization to explore whether a preformed AP axis, which could be implicated by the asymmetric localization of *Aphb* and *Apcad* mRNAs, existed in the sexual oocytes.

In comparison with asexual (viviparous) ovarioles (Fig. 5A), the sexual ovarioles have fewer egg chambers, usually 1–3 per ovariole, but the germaria and oocytes are up to fivefold larger (Fig. 5B–D, G–J). In asexual ovarioles, *Aphb* mRNA was expressed in the germaria and localized to the anterior pole of developing oocytes as well as to the egg chambers accommodating early embryos (stage 3 in Fig. 5A) (Huang *et al*., 2010). Nevertheless, while anterior localization of *Aphb* was detected, concurrent localization of *Apcad* mRNA in the posterior region

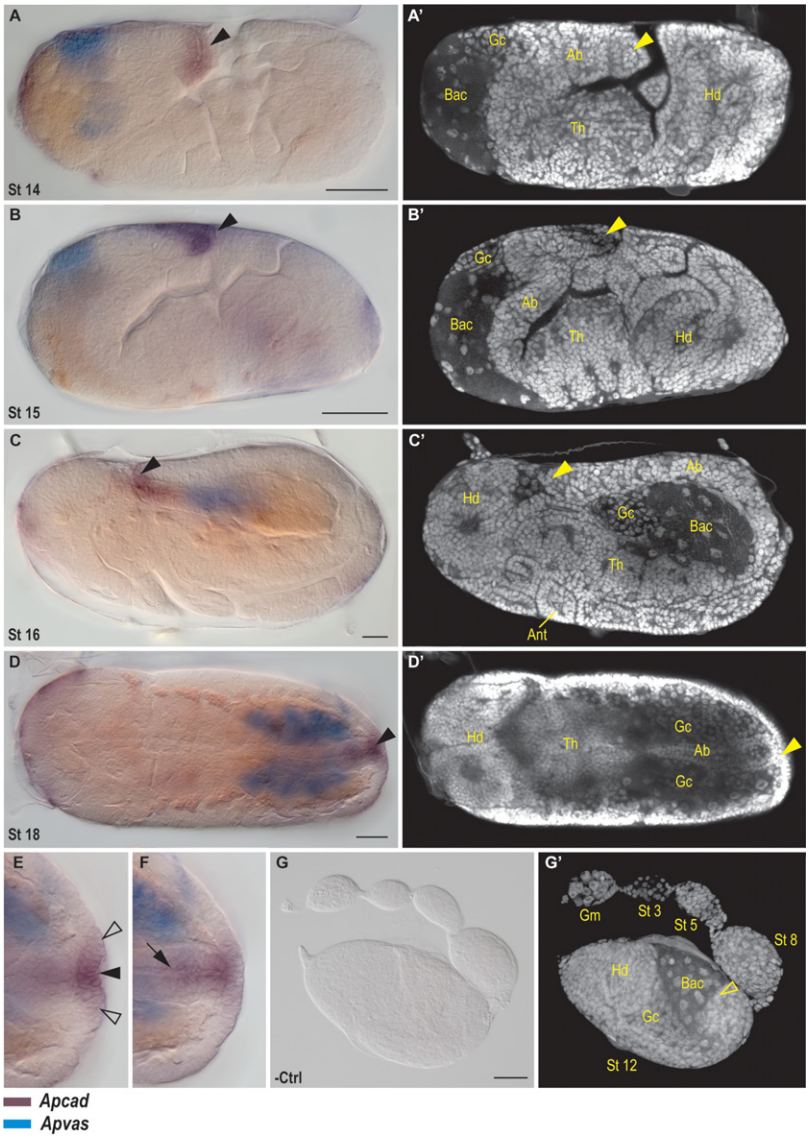

Figure 4. Developmental expression of *Apcad* mRNA before and after katatrepsis (embryo flip). Dissected ovarioles were hybridized with digoxigenin (DIG)-labelled *Apcad* and fluorescein-labelled *Apvas1* antisense riboprobes concurrently. Colour keys indicating expression signals of *Apcad* and *Apvas1* are shown under the figure. Anterior region of egg chambers is to the left; dorsal is upper. Before katatrepsis, the embryonic head is located in the egg posterior; after katatrepsis, it is located in the egg anterior. All views are lateral except those in panels (D) to (F), where embryos are presented dorsally. Panels (A′) to (D′) and panel (G′) are nuclear stains of preparations shown in panels (A) to (D) and panel (G), respectively. (A) Extending germ band prior to katatrepsis (stage 14). (B) Initiation of katatrepsis (stage 15). (C) Completion of katatrepsis (stage 16). (D) Germ band retraction completed (stage 18). Expression of *Apcad* was detected in the posteriormost region of the germ band (arrowheads). In (D), the *Apcad* expression observed in the anteriormost region was non-specific signals in the extraembryonic membrane associated with the head. (E, F) Magnification of the posterior region displayed in (D). Images in panels (E) and (F) are shown at different focal planes. In (E), the arrowhead designates the preferential expression of *Apcad* in the central region of the last abdominal segment; hollow arrowheads label the weak expression in the adjacent area. In (F), arrow indicates the anterior boundary of the *Apcad* expression in the invaginating proctodeum (hindgut). (G) Negative control (-Ctrl). Ovarioles were hybridized with a DIG-labelled sense riboprobe of *Apcad*. No signals were detected. Abbreviations: Ab, abdomen; Ant, antenna; Bac, bacteria; Gc, germ cells; Hd, head; Th, thorax; St, stages. Scale bar, 20 μm.

was not identified. The first appearance of *Apcad* expression in the egg posterior was not detected until the anterior localization of *Aphb* became almost undetectable in the blastula (stage 6 in Fig. 5A). Using the same *in situ* hybridization conditions for detecting *Apcad* expression in asexual ovarioles (Fig. 5E), we did not identify *Apcad* mRNA expressed in the sexual ovarioles (Fig. 5B, C). In effect, our RT-PCR results showed that expression of *Apcad* was not detectable in the sexual ovaries dissected from the adult females (Fig. 5F). As in asexual ovarioles, we found that expression of *Aphb* mRNA was localized to the anterior pole of the previtellogenic oocytes in the sexual ovarioles (Fig. 5G). From vitellogenesis onward, we could even identify an AP gradient of *Aphb* in the anterior one fifth of the oocyte length (Fig. 5H). Additionally, in the sexual oocytes we did not identify localization patterns of *Apvas1* or *Apnos1*, both of which are known to be germline-specific in asexual embryos (Chang *et al.*, 2007, 2009; Shigenobu *et al.*, 2010). Transcripts of *Apvas1* and *Apnos1* were evenly distributed in the previtellogenic (not shown) and vitellogenic oocytes (Fig. 5I, J).

Morphological structures of sexual ovarioles are presented and annotated in Fig. 5B′. An outline of *Apcad* expression during embryogenesis in the asexual pea aphid is shown in Fig. 6.

Discussion

Most of the developmental genes involved in *Drosophila* segmentation are conserved among arthropods, but their hierarchical positions in the segmentation cascade show

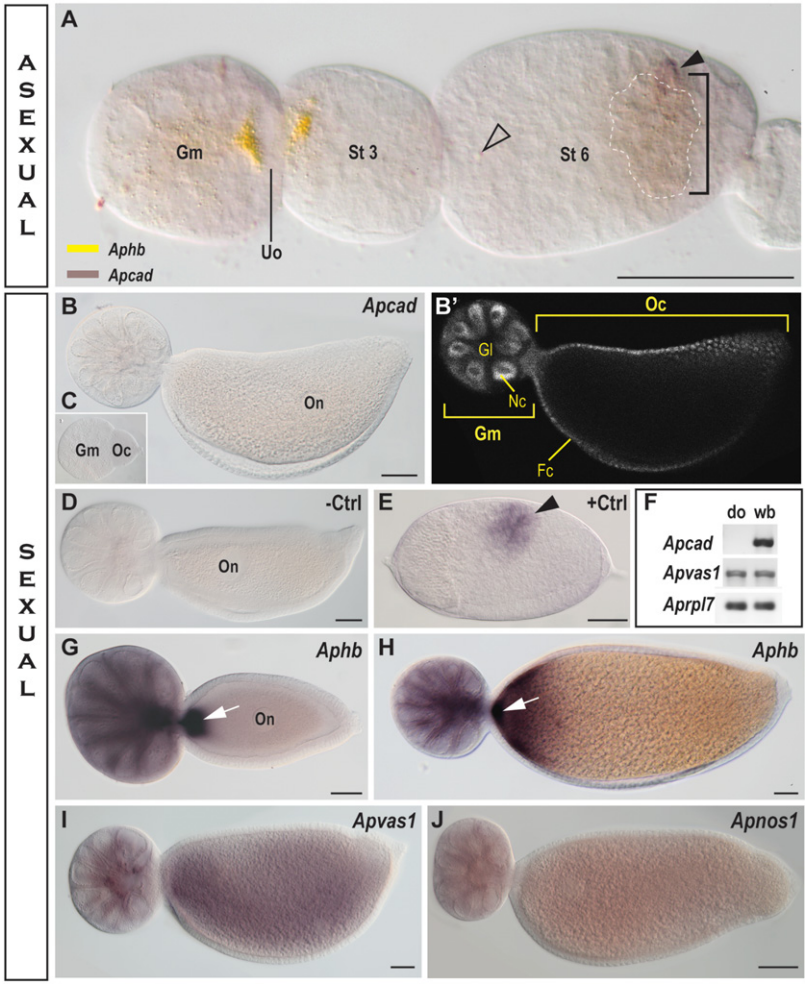

Figure 5. Comparison of *Aphb* and *Apcad* expression between asexual and sexual ovarioles. All ovarioles were dissected from female adults. Anterior is to the left for all ovarioles; dorsal is up for the embryo shown in (E). (A): asexual ovarioles; (B)–(D) and (G)–(J): sexual ovarioles; (E): a stage-11 asexual embryo. Except ovarioles in (C) and (G), which are previtellogenic, all sexual ovarioles presented in this figure are vitellogenic. (A) Asexual ovarioles hybridized with antisense riboprobes of fluorescein-labelled *Aphb* and digoxigenin (DIG)-labelled *Apcad*. *Aphb* mRNA was localized to the anterior part of the unsegregated oocytes and uncellularized embryos (shown as the stage-3 embryo). In stage-6 embryos, where the cellular blastoderm is formed, anterior localization of *Aphb* is almost not identified (hollow arrowhead). Expression of *Apcad* mRNA, as shown in Figure 2, was detected in the posterior region of stage-6 embryos (bracket). The arrowhead indicates the preferential expression of *Apcad*. Primordial germ cells (PGCs) with weak expression of *Apcad* are marked with dashed lines. Compared with Figure 2F, *Apcad* signals in PGCs were further down-regulated here in a late stage-6 embryo. *In situ* signals of *Apcad* and *Aphb* are indicated with colour keys. (B, C) Sexual ovarioles hybridized with antisense riboprobes of DIG-labelled *Apcad*. (B′) is nuclear staining of (B). Transcripts of *Apcad* were not identified in either previtellogenic (B) or vitellogenic ovarioles (C). (D) Negative control (-Ctrl). Ovarioles were hybridized with a DIG-labelled sense riboprobe of *Apcad*. No signals were detected. (E) Positive control (+Ctrl). Asexual ovarioles were hybridized with the same batch of *Apcad* probes used in sexual *in situs* of (B) and (C), demonstrating that *Apcad* can mark the posteriormost region (arrowhead) of germ band. (F) Comparison of *Apcad* expression between dissected ovarioles (do) and whole bodies (wb) of sexual adult females using reverse transcription PCR. Expression of *Apcad* was not detected in sexual ovarioles but it was detected in RNA extracted from whole organisms. *Apvas1*, positive control; *Aprpl7*, internal control. (G, H) Sexual ovarioles hybridized with antisense riboprobes of DIG-labelled *Aphb*. In both previtellogenic (G) and vitellogenic (H) ovarioles, expression of *Aphb* mRNA could be detected in germaria and anterior region of oocytes. In (G), anterior localization of *Aphb* (arrow) was restricted to the anterior pole. In (H), expression of *Aphb* formed an anteroposterior gradient in the anterior one-fifth of the oocytes. *Aphb* mRNA localized to the anterior pole was indicated with arrows. (I, J) Sexual ovarioles hybridized with antisense riboprobes of DIG-labelled *Apvas1* (I) and *Apnos1* (J), respectively. Expression of *Apvas1* and *Apnos1* mRNA was identified in the germaria and oocytes. Abbreviations: Fc, follicle cells; Gl, germarial lumen; Gm, germaria; Nc, nurse cells; Oc, oocytes; On, oocyte nuclei; St, stages; Uo, un-segregated oocytes. Scale bar, 40 μm.

much diversity among different lineages. It is clear that the relative conservation of developmental genes fits an 'hourglass model', where the width of the hourglass is inversely proportional to the degree of conservation: maternal genes for axis determination, which are at the top of the cascade, have the least conservation; following maternal genes, the conservation index increases for gap genes, then pair-rule genes, and is highest in the segment

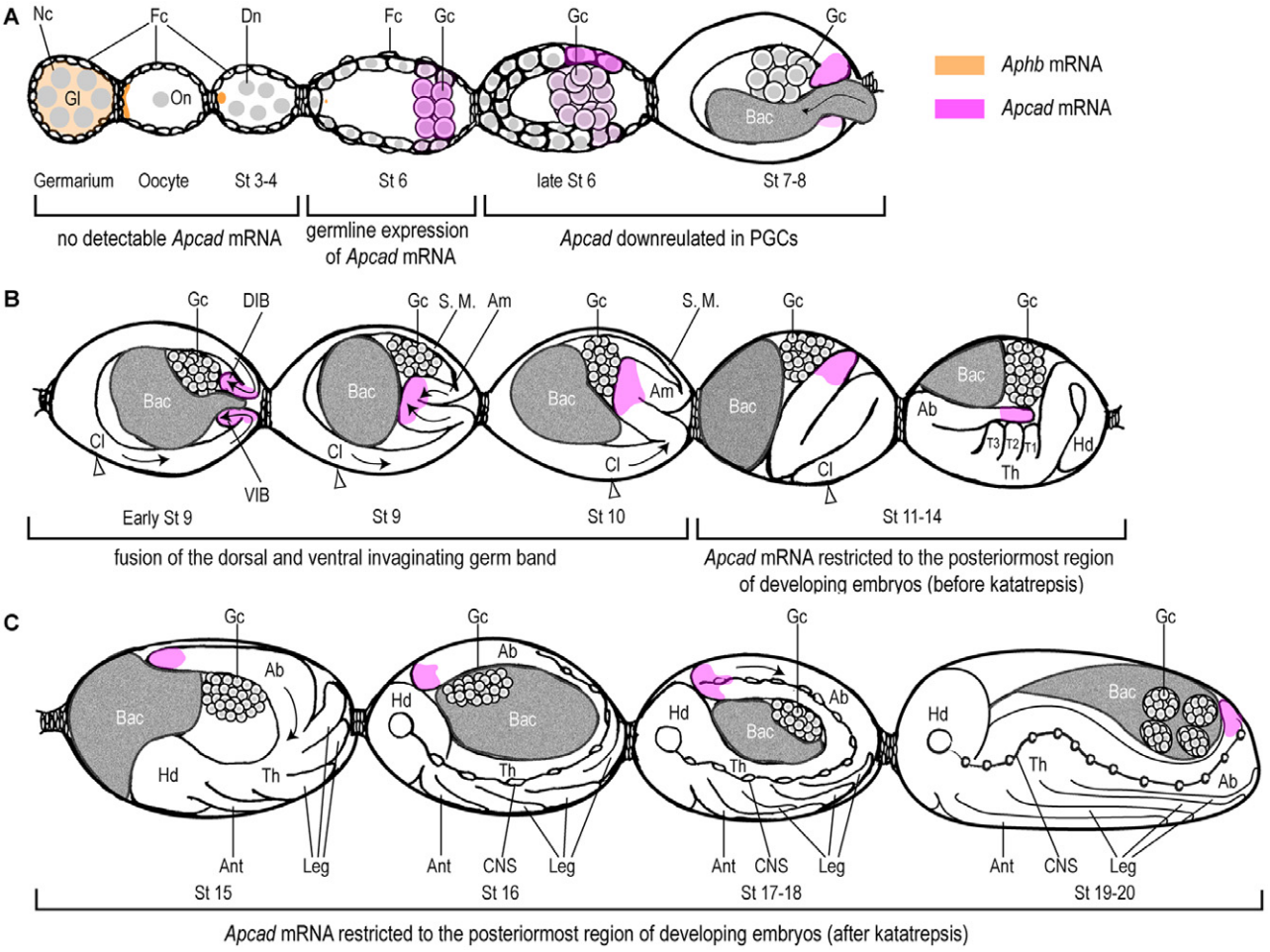

Figure 6. Schematic illustration of *Apcad* expression during embryogenesis of the asexual pea aphid. Expression patterns of *Apcad* are illustrated according to staining results shown in Figs 1–5; staging of embryos is based upon morphological characteristics described by Miura *et al.* (2003). Anterior localization of *Aphb* is highlighted in embryos before stage 6 of development but *Aphb* expression in later stages, which is not anteriorly localized, is omitted. *In situ* signals of *Apcad* and *Aphb* are indicated with colour keys. For all egg chambers, anterior is to the left and dorsal is uppermost; embryos are presented laterally. The anterior–posterior (AP) axis in embryos between stages 11–14 is opposite to the AP orientation of the egg chambers. (A) Germaria, oocytes and early embryos (stages 0–8). We did not detect *Apcad* signals in germaria, oocytes, stages 0–4 embryos, and stage-5 embryos with few newly segregated cells in the posteriormost region of the blastoderm (data not shown). *Apcad* expression was first identified in germ cells and their surrounding blastoderm in the posterior region of the blastula (stage 6). Expression of *Aphb* was detected in the anterior pole of egg chambers from stages 0–5 but anterior localization of *Aphb* became nearly undetectable in the stage-6 embryos. During late blastulation (late stage 6), *Apcad* expression was down-regulated in the proliferating germ cells but it was elevated in the posterior blastoderm located dorsally. Asymmetric distribution of *Apcad* transcripts was detected in the stage 7–8 embryos: preferential expression of *Apcad* was restricted to the dorsal invaginating blastoderm while weaker expression was detected in the posterior ventral blastoderm prior to invagination. Arrow indicates the migration of endosymbionts. (B) Gastrulation, formation of the closed blastopore, and germ band extension (stages 9–14). *Apcad*-positive signals were located in both the dorsal and ventral invaginating germ band (stage 9). The exact timing of germ band fusion remains uncertain but the formation of the closed blastopore is completed in stage-10 embryos and, according to our data and Will (1888), the fused invaginating germ band expressing *Apcad* later becomes the growth zone in the stage-11 embryos. Arrows indicate the movement of the cephalic lobes and the invaginating germ band (Will, 1888; Huang *et al.*, 2010). (C) Embryos during and after katatrepsis (stages 15–20). *Apcad* expression was restricted to the posteriormost region of the abdomen, regardless of the orientation of the embryos. Arrow indicates the contraction of the germ band. Abbreviations: Ab, abdomen; Am, amnion; Ant, antenna; Bac, bacteria; Cl, cephalic lobe; CNS, central nervous system; DIB, dorsal invaginating blastoderm; Dn, dividing nuclei; Fc, follicle cells; Gc, germ cells; Gl, germarial lumen; Hd, head; Nc, nurse cells; On, oocyte nucleus; S. M., serosal membrane (serosa); St, stages; Th, thorax; T1-T3, thoracic segments 1 to 3; VIB, ventral invaginating blastoderm.

polarity genes at the midpoint of the hourglass; the degree of conservation then decreases again in homeotic (*Hox*) genes that are involved in the specification of axial identities (Duboule, 1994; Peel *et al.*, 2005; Kalinka *et al.*, 2010). This model suggests that genes functioning before blastoderm formation (maternal genes, gap genes) are less conserved than those functioning in a cellularized germ band undergoing segmentation (pair-rule genes, segment polarity genes). In this study we find that the expression of *Apcad* mRNA matches this evolutionary

trend: *Apcad* expression prior to gastrulation differs in comparison to *cad* expression as described in other insects; after gastrulation, however, restriction of *Apcad* mRNA to the posteriormost region of the germ band adheres to the canonical role of *cad* genes in insects and other arthropods (Figs 3–5; 6B, C). In the following paragraphs we discuss the noncanonical patterns of *Apcad* expression and propose potential roles for *Apcad* during posterior development in the pea aphid.

In *Drosophila* (Mlodzik & Gehring, 1987), *Nasonia* (wasp; Olesnicky *et al*., 2006), *Bombyx* (silkworm; Xu *et al*., 1994), and *Apis* (honeybee; Wilson *et al*., 2010), all of which are insects containing polytrophic ovarioles, expression of *cad* mRNA can be identified in the cytoplasm of both nurse cells and oocytes. In addition to the polytrophic ovarioles, the presence of maternal *cad* mRNA in the telotrophic ovarioles of *Tribolium* (beetle) as well as in the panoistic ovarioles of *Schistocerca* (grasshopper) and *Gryllus* (cricket) has also been reported (Schulz *et al*., 1998; Dearden & Akam, 2001; Shinmyo *et al*., 2005). Functional analyses show that maternal *cad* mRNA deposited in the oocytes is involved in axis elongation and segmentation in early embryos of *Drosophila*, *Nasonia*, *Tribolium* and *Gryllus* (Mlodzik & Gehring, 1987; Shinmyo *et al*., 2005; Olesnicky *et al*., 2006; Schoppmeier *et al*., 2009). In contrast, the absence of *Apcad* mRNA in nurse cells and oocytes of the asexual pea aphid is exceptional (Figs 2A; 6A), indicating that *Apcad* does not play a role in early patterning. This inference is supported by the continuous absence of *Apcad* expression in early embryos prior to blastoderm formation (Figs 2B, E; 6A). After gastrulation, however, expression of *Apcad* mRNA is restricted to the growth zone of the elongating germ band, suggesting that *Apcad* conserves the canonical role of *cad* genes in axis elongation from mid-embryogenesis onward in the asexual pea aphid (Figs 3C; 4A–C; 6B, C).

The pea aphid becomes the third insect model, after *Drosophila* and *Nasonia*, in which germline expression of *cad* can be identified (Fig. 2C). One common feature of these three species is that specification of germ cells depends on a preformed germ plasm in the posterior region of the egg, but localization of *cad* mRNA to the germ plasm can only be found in *Nasonia* (Olesnicky *et al*., 2006). In *Drosophila* (Mlodzik & Gehring, 1987) and pea aphid (Figs 2C; 6A), *cad* mRNA is not particularly restricted to the germ plasm and germline expression of *cad* is first detected in the newly formed PGCs. However, whether *cad* is involved in the assembly of the germ plasm in *Nasonia* and whether *cad* is required for germline development in *Drosophila* remain unclear. In *Nasonia*, knockdown of *cad* through parental RNAi can cause laying of fewer eggs, implicating a role for *cad* in oogenesis (Olesnicky *et al*., 2006). In *Drosophila*, we have not found reports describing how germline development is affected in maternal (cad^{mat}) or zygotic (cad^{zyg}) mutants for *cad*. This may be attributable to partial rescue between maternal and zygotic *cad* mRNA driven by different promoters (Mlodzik & Gehring, 1987); nonetheless, PGC development is seriously retarded in $cad^{mat+zyg}$ mutants owing to severe defects in the abdomen (Macdonald & Struhl, 1986). With regard to aphids, we have not been successful in silencing the embryonic expression of *Apcad* using RNAi, hence whether *Apcad* can regulate the early development of PGCs remains an open question.

In *Drosophila*, a high concentration of Hb protein in the anterior region inhibits the expression of *cad* mRNA whereas a lower concentration of Hb in one half of the egg posterior allows the formation of the *cad* abdominal domain (Schulz & Tautz, 1995). Similarly, *hb* prevents the expansion of *cad* expression to the anterior in *Nasonia* (Olesnicky *et al*., 2006). Taken together, this suggests that inhibition of *cad* expression by *hb* is a conserved mechanism in insects. In the asexual pea aphid, *Apcad* expression in the posterior region of the egg is first detectable just as anterior localization of *Aphb* vanishes (Huang *et al*., 2010), implying that maternal *Aphb* plays a conserved role in suppressing the expression of *Apcad* (Figs 5A; 6A). We hypothesize that the inhibition of *Apcad* expression is achieved by the ApHb protein expressed in germaria as well as early embryos prior to blastulation (Supplementary Fig. S1A). The transcriptional inhibition of *Apcad* may be largely suppressed by ApHb in the germarium, from which maternal transcripts are synthesized and transported to oocytes and early embryos via the trophic cord (Blackman, 1978). This is why transcripts of *Apcad* cannot be detected in germaria and embryos prior to blastulation (Fig. 2A, B, and E). Nevertheless, we cannot exclude the possibility that residual expression of *Apcad* is inhibited by ApHb within oocytes and early embryos in the asexual pea aphid.

The lack of *Apcad* expression prior to blastoderm formation in the asexual pea aphid indicates that *Apcad* has lost the ancestral functions of *cad* in regulating gap genes during early embryogenesis. This ancestral 'master organizer of patterning' role of *cad* has been reported in *Nasonia* (Olesnicky *et al*., 2006), *Gryllus* (Shinmyo *et al*., 2005), *Tribolium* (Schoppmeier *et al*., 2009), and *Artemia franciscana* (brine shrimp) (Copf *et al*., 2004). For example, in *Gryllus*, *cad* activates the gap genes *hb* and *Krüppel* (*Kr*) to form gnathal and thoracic segments (Shinmyo *et al*., 2005); in *Nasonia*, *cad* positions the posterior boundary of the anterior domain of *hb* via activating *Kr* expression (Olesnicky *et al*., 2006). Recently, expression of *Ap-Kr* has been identified in germaria, oocytes, and early embryos prior to blastulation (Duncan *et al*., 2013), all of which are locations devoid of *Apcad* staining in the asexual pea aphid (Fig. 2A, B). This suggests that *Apcad*, in contrast to

the functions of *cad* in *Gryllus and Nasonia*, may not regulate the expression of *Ap-Kr*. *Apcad* might, of course, commence to regulation of gap genes after it is expressed from germ band extension onward in the asexual embryos. With regard to the potential roles of *Apcad* in sexual embryos, we have not yet obtained expression data of *Apcad* and other gap genes during sexual development and so can make no observations. Apart from the pea aphid, the loss of maternal *cad* expression in the lower cyclorrhaphan fly *Megaselia abdita* is so far the only case reported among published insect models (Stauber *et al*., 2008). Consequently, we would like to extend our study of *cad* genes to other aphid species, as well as to other hemipterans, to understand whether the loss of ancestral roles for *cad* during early development is a universal phenomenon among aphids or if it is even the norm in Hemiptera.

The absence of *Apcad* expression in early embryos indicates that *Apcad* is unlikely to be a posterior organizer in the asexual pea aphid. Similarly, *Apotd*, an orthologue of *otd* genes in the pea aphid (Huang *et al*., 2010), does not act as an anterior organizer because expression of *Apotd* mRNA, like *Apcad* mRNA, cannot be detected in early embryos prior to blastoderm formation. In contrast, the anterior and posterior organizers *otd* and *cad* have been identified in long-germ insects such as *Nasonia* (Lynch *et al*., 2006; Olesnicky *et al*., 2006) and short-germ insects such as *Gryllus* (Shinmyo *et al*., 2005; Nakamura *et al*., 2010), *Tribolium* (Copf *et al*., 2004; Kotkamp *et al*., 2010), and *Bombyx* (Nakao, 2012). This suggests that *otd* and *cad* retain their ancestral roles in directing AP patterning in most insects but some of their functions during early embryogenesis have been taken over by *bcd* and *osk* in highly derived species such *Drosophila*. If *otd* and *cad* do not act as AP organizers in the asexual pea aphid and if this species does not possess homologues of *bcd* and *osk* (Shigenobu *et al*., 2010), which genes can specify the AP development remains an open question. At present, we infer that *Aphb* is a potential anterior organizer because anterior localization of *Aphb* mRNA in oocytes and early embryos resembles the localization patterns of *bcd* in *Drosophila*, although *hb* and *bcd* are not homologous to each other (Huang *et al*., 2010). Localized Nos signals that were detected by a cross-reacting antibody in the posterior region of early embryos support the idea that *nos* might retain its conserved role as a posterior organizer in the asexual pea aphid (Chang *et al*., 2006). Among the four *nos* genes in the pea aphid we have so far not been able to identify which one confers the localized signals. Nevertheless, the noncanonical expression patterns of *Apcad* and *Apotd* strongly suggest that mechanisms involved in AP axis formation in the asexual pea aphid has been reprogrammed at the top level of the segmentation hierarchy.

Experimental procedures

Pea aphid culture

The parthenogenetic and viviparous pea aphids (*Acyrthosiphon pisum*) were derived from an obligate parthenogenetic clone in Taiwan, maintained on garden pea plants (*Pisum sativum*) at 20 °C in a growth chamber under a 16 h light/8h dark regime for >200 generations. Staging of embryonic development of the asexual embryos followed the scheme described by Miura *et al*. (2003). The local obligate parthenogenetic strain was used for cloning and *in situ* hybridization of *Apcad*, but this clone is obligately parthenogenetic and cannot be induced to reproduce sexually. We therefore detected the expression of *Apcad* mRNA in sexual ovaries dissected from the ApL strain maintained in Japan. Induction of sexual morphs was conducted under short-day conditions (8h light/16h dark). Details of induction were those described by Ishikawa *et al*. (2012). For both local and ApL strains, we sequenced 451 nucleotides of *Apcad* cDNA that were used as templates for synthesizing riboprobes. We compared *Apcad* sequences from three pea aphid strains: local (Taipei), ApL, and LSR1.AC.G1 (the aphid strain used for whole genome sequencing) (The International Aphid Genomics Consortium, 2010), and found that the sequences of the 451 nucleotides were all identical. This suggests that *Apcad* coding sequences are highly conserved among the pea aphid strains.

Cloning and reverse transcription-PCR of Apcad

Total RNA was extracted from dissected ovarioles of asexual and sexual adult pea aphids using the RNeasy Mini Kit (Qiagen, Hilden, Germany). Purified RNA was reverse transcribed into cDNA with poly dT_{18} primers and StrataScript Reverse Transcriptase (Stratagene, La Jolla, CA, USA). RNA extraction and reverse transcription experiments were performed according to the manufacturers' instructions. Degenerate primers for PCR cloning were designed to match the conserved motifs flanking the homeobox sequences of Cad (Caudal)/Cdx (Cad-related homeobox) proteins: forward primer, 5′-ACCCGCACCAAGGATA AGTAC(A/C)G(A/C/G/T)GT(A/C/G/T)GT(A/C/G/T)TA-3′ (encoding TRTKDKYRVV); reverse primer, 5′-CGGCGGTTCTGGAACC A(A/G/T)AT(C/T)TT-3′ (encoding KIWFQNR). Experiments using 5′ RACE-PCR were performed using the GeneRacer kit (Invitrogen, Carlsbad, CA, USA). Primers for RACE-PCR were: (1) 5′ RACE: forward primer, 5′-CGACTGGAGCACGAGGACA CTGA-3′ (GeneRacer™ 5′ primer); forward nested primer, 5′-GGACACTGACATGGACTGAAGGAGTA-3′ (GeneRacer™ 5′ nested primer); reverse primer, 5′-GCGGTCGAATATAAGCTC ATATCG-3′ (located in the 3′ untranslated region (Fig. 1B)); reverse nested primer, 5′-AGGCTCAGCATTTTGGAC-3′ (encoding LSKMLSL); (2) 3′-RACE PCR: forward primer, 5′-TATACACCGACTTGCAGCG-3′ (encoding VYTDLQR); forward nested primer, 5′-AACCGATACATCACGATCAC-3′ (encoding NRYITI); reverse primer, 5′-GCTGTCAACGATACG CTACGTAACG-3′ (GeneRacer™ 3′ primer); reverse nested primer, 5′-CGCTACGTAACGGCATGACAGTG-3′ (GeneRacer™ 3′ nested primer). Sequences were aligned using MacVector version 7.2.2 (Accelrys Inc., San Diego, CA, USA).

The RT-PCR was performed using cDNA reverse transcribed from RNA of ovarian and somatic tissues. Egg chambers in the asexual ovarioles were separated with a black enameled pin (diameter: 0.25 mm; Entomoravia, Slavkov u Brna, Czech

Republic). Dissection was on the follicular stalks between egg chambers younger/older than stage 5 of development (a developmental stage with morphologically identifiable PGCs) (Miura *et al*., 2003). Total RNA was extracted from germaria and dissected egg chambers of 10 adults (equivalent to 120~140 ovarioles) using the EasyPure Total RNA Reagent TRI-100 (Bioman, Taipei, Taiwan). Input quantity of total RNA for each RT reaction (20 μl) was 0.6 μg, reverse transcribed with HiScript I reverse transcriptase (Bionovas, Toronto, Canada) and poly dT_{18} primers. cDNA in 1 μl of the RT products served as template for a PCR reaction (10 μl; condition: 94 °C for 5 min, followed by 29 cycles at 94 °C for 30 s, 60 °C for 30 s, 72 °C for 1 min and, finally, 72 °C for 10 min). RNA extraction and RT-PCR on sexual aphids followed the same conditions performed in the asexual morphs. Gene-specific primers designed for the RT-PCR were: *Apcad*: 5′-ACTGGCCACCCGTACAGCAGC-3′ (forward), 5′-GCGGTCG AATATAAGCTCATATCG-3′ (reverse), amplicon: 451 bp; *Apvas1*: 5′-ATGTCTGACGGTGGTTGGGATG-3′ (forward), 5′-GGGCAG TAGCCATCATATCTCGTC-3′ (reverse), amplicon: 616 bp, positive control (Chang *et al*., 2007); *ribosomal protein like 7* (*Aprpl7*): 5′-AATCAAGGGACAACGCATTCC-3′ (forward), 5′-ATTGGTCT TCTTACGCCAGCCTCC-3′ (reverse), amplicon: 193 bp, internal control (Nakabachi *et al*., 2005).

Whole-mount in situ *hybridization and histology*

We transcribed antisense and sense riboprobes of *Apcad*, *Aphb*, and *Apvas1* using linearized plasmids as templates. Sequences of *Apcad* riboprobes were equivalent to those amplified by RT-PCR as above. Riboprobes of *Aphb* and *Apvas1* were synthesized according to the methods described in Huang *et al*. (2010) and Chang *et al*. (2007). Digoxigenin (DIG)-labelled uridine triphosphates were incorporated into the *Apcad* probes using the DIG RNA Labeling Kit (SP6/T7; Roche, Basel, Switzerland). An antisense riboprobe of *Aphb* used in single and double *in situ* assays was labelled with the Fluorescein (FLU) Labeling Mix (Roche), as was the *Apvas1* antisense riboprobe added to the double *in situs*. Hybridization was carried out at 68 °C overnight for all riboprobes used in this study.

All riboprobes labeled with DIG/FLU uridine triphosphates were detected with anti-DIG/FLU Fab fragments conjugated with alkaline phosphatase. For single *in situs* of *Apcad* (Fig. 2A-C, F-H′), *Aphb* (Fig. 5G, H), *Apvas1* (Fig. 5I), and *Apnos1* (Fig. 5J), we developed signals with the substrate Nitroblue tetrazolium (NBT)/5-bromo-4-chloro-3-indolyl phosphate (BCIP; Roche). Substrate combinations for double *in situ* assays were designed as follows: (1) *Apcad*, NBT/BCIP; *Apvas1*, 4-benzoylamino-2,5-diethoxybenzenediazonium chloride hemi[zinc chloride] (Fast Blue BB) salt/naphthol-AS-MXphosphate (NAMP; Sigma, St. Louis, MO, USA) (Figs 2F′; 3; 4); (2) *Apcad*, NBT/BCIP; *Aphb*, 2-[4-Iodophenyl]-3-[4-nitrophenyl]-5-phenyl-tetrazolium chloride (INT)/BCIP (Sigma) (Fig. 5A). Concentrations of substrates and protocols for *in situ* hybridizations followed Chang *et al*. (2008). Nuclear counterstaining was carried out with DAPI (2 ng/ml; Sigma). We produced Nomarski images of each sample preparation using a Leica DMR (Leica, Wetzlar, Germany) connected to a Canon EOS 5D MarkII digital camera (Canon, Tokyo, Japan). Photos of DAPI staining were taken with the C-Apo 40X/1.2 water lens linked to a Zeiss LSM510 META laser-scanning microscope (Carl Zeiss, Jena, Germany).

Acknowledgements

We thank Sue-Ping Lee for technical support on confocal microscopy, Hsiao-Ling Lu and Nai-Wei Jiang for *in situ* hybridization and immunostaining, Kota Ogawa and Miyuzu Suzuki for RNA extraction and dissection of ovaries from sexual aphids, and Chen-Yo Chung, Nai-Wei Jiang, Gee-Way Lin and Hsiao-Ling Lu for critical reading of the manuscript. This work was supported by the National Science Council (101–2313-B-002–059-MY3 and 101–2321-B-002–090-MY2 for C-c.C.; 8–2311-565-B-001–015-MY3 and 101–2311-B-001–005 for T.H.C.), Academia Sinica (Short-term Domestic Visiting Scholarship (2010) for C-c.C.; Academia Sinica's Thematic Project (AS-99-TP-B20) for T.H.C.), BAPHIQ of the Agricultural Council (101.10.2.1-B3(4)), and National Taiwan University (NTU-CESRP 101R4602D3 and 102R7602D3).

References

Blackman, R.L. (1978) Early development of parthenogenetic egg in three species of aphids (Homoptera Aphididae). *Int J Insect Morphol* **7**: 33–44.

Chang, C-C., Lin, G.W., Cook, C.E., Horng, S.B., Lee, H.J. and Huang, T.Y. (2007) *Apvasa* marks germ-cell migration in the parthenogenetic pea aphid *Acyrthosiphon pisum* (Hemiptera: Aphidoidea). *Dev Genes Evol* **217**: 275–287.

Chang, C-C., Lee, W.C., Cook, C.E., Lin, G.W. and Chang, T. (2006) Germ-plasm specification and germline development in the parthenogenetic pea aphid *Acyrthosiphon pisum*: Vasa and Nanos as markers. *Int J Dev Biol* **50**: 413–421.

Chang, C-C., Huang, T.Y., Shih, C.L., Lin, G.W., Chang, T.P., Chiu, H. *et al*. (2008) Whole-mount identification of gene transcripts in aphids: protocols and evaluation of probe accessibility. *Arch Insect Biochem Physiol* **68**: 186–196.

Chang, C-C., Huang, T.Y., Cook, C.E., Lin, G.W., Shih, C.L. and Chen, R.P. (2009) Developmental expression of *Apnanos* during oogenesis and embryogenesis in the parthenogenetic pea aphid *Acyrthosiphon pisum*. *Int J Dev Biol* **53**: 169–176.

Copf, T., Schröder, R. and Averof, M. (2004) Ancestral role of *caudal* genes in axis elongation and segmentation. *Proc Natl Acad Sci USA* **101**: 17711–17715.

Dearden, P.K. and Akam, M. (2001) Early embryo patterning in the grasshopper, *Schistocerca gregaria*: *wingless*, *decapentaplegic* and *caudal* expression. *Development* **128**: 3435–3444.

Duboule, D. (1994) Temporal colinearity and the phylotypicprogression: a basis for the stability of a vertebrate Bauplan and the evolution of morphologies through heterochrony. *Development* **Suppl**: 135–142.

Duncan, E.J., Leask, M.P. and Dearden, P.K. (2013) The pea aphid (*Acyrthosiphon pisum*) genome encodes two divergent early developmental programs. *Dev Biol* **377**: 262–274.

Ewen-Campen, B., Srouji, J.R., Schwager, E.E. and Extavour, C.G. (2012) *Oskar* predates the evolution of germ plasm in insects. *Curr Biol* **22**: 2278–2283.

Extavour, C.G. (2011) Long-lost relative claims orphan gene: *oskar* in a wasp. *Plos Genet* **7**: e1002045.

Fu, J., Posnien, N., Bolognesi, R., Fischer, T.D., Rayl, P., Oberhofer, G. *et al*. (2012) Asymmetrically expressed *axin* required for anterior development in *Tribolium*. *Proc Natl Acad Sci U S A* **109**: 7782–7786.

Gonzalez-Reyes, A., Elliott, H. and St Johnston, D. (1995) Polarization of both major body axes in *Drosophila* by *gurken-torpedo* signalling. *Nature* **375**: 654–658.

Hagan, H.R. (1951) Chapter 13. Pseudoplacental viviparity-Corrodentia, Hemiptera (Aphididae). In *Embryology of the Viviparous Insects*, pp. 347–392. Roland Press, New York.

Huang, T.Y., Cook, C.E., Davis, G.K., Shigenobu, S., Chen, R.P. and Chang, C-C. (2010) Anterior development in the parthenogenetic and viviparous form of the pea aphid, *Acyrthosiphon pisum*: *hunchback* and *orthodenticle* expression. *Insect Mol Biol* **19** (Suppl 2): 75–85.

Ishikawa, A., Ogawa, K., Gotoh, H., Walsh, T.K., Tagu, D., Brisson, J.A. *et al*. (2012) Juvenile hormone titre and related gene expression during the change of reproductive modes in the pea aphid. *Insect Mol Biol* **21**: 49–60.

Kalinka, A.T., Varga, K.M., Gerrard, D.T., Preibisch, S., Corcoran, D.L., Jarrells, J. *et al*. (2010) Gene expression divergence recapitulates the developmental hourglass model. *Nature* **468**: 811–814.

Kotkamp, K., Klingler, M. and Schoppmeier, M. (2010) Apparent role of *Tribolium orthodenticle* in anteroposterior blastoderm patterning largely reflects novel functions in dorsoventral axis formation and cell survival. *Development* **137**: 1853–1862.

Kugler, J.M. and Lasko, P. (2009) Localization, anchoring and translational control of *oskar*, *gurken*, *bicoid* and *nanos* mRNA during *Drosophila* oogenesis. *Fly (Austin)* **3**: 15–28.

Lall, S. and Patel, N.H. (2001) Conservation and divergence in molecular mechanisms of axis formation. *Annu Rev Genet* **35**: 407–437.

Lall, S., Ludwig, M.Z. and Patel, N.H. (2003) Nanos plays a conserved role in axial patterning outside of the Diptera. *Curr Biol* **13**: 224–229.

Langdon, Y.G. and Mullins, M.C. (2011) Maternal and zygotic control of zebrafish dorsoventral axial patterning. *Annu Rev Genet* **45**: 357–377.

Lynch, J.A. and Desplan, C. (2003) 'De-evolution' of *Drosophila* toward a more generic mode of axis patterning. *Int J Dev Biol* **47**: 497–503.

Lynch, J.A. and Desplan, C. (2010) Novel modes of localization and function of *nanos* in the wasp *Nasonia*. *Development* **137**: 3813–3821.

Lynch, J.A., Brent, A.E., Leaf, D.S., Pultz, M.A. and Desplan, C. (2006) Localized maternal *orthodenticle* patterns anterior and posterior in the long germ wasp *Nasonia*. *Nature* **439**: 728–732.

Lynch, J.A., Ozuak, O., Khila, A., Abouheif, E., Desplan, C. and Roth, S. (2011) The phylogenetic origin of *oskar* coincided with the origin of maternally provisioned germ plasm and pole cells at the base of the Holometabola. *Plos Genet* **7**: e1002029.

Macdonald, P.M. and Struhl, G. (1986) A molecular gradient in early *Drosophila* embryos and its role in specifying the body pattern. *Nature* **324**: 537–545.

McGregor, A.P., Pechmann, M., Schwager, E.E. and Damen, W.G. (2009) An ancestral regulatory network for posterior development in arthropods. *Commun Integr Biol* **2**: 174–176.

Miura, T., Braendle, C., Shingleton, A., Sisk, G., Kambhampati, S. and Stern, D.L. (2003) A comparison of parthenogenetic and sexual embryogenesis of the pea aphid *Acyrthosiphon pisum* (Hemiptera: Aphidoidea). *J Exp Zool* **295B**: 59–81.

Mlodzik, M. and Gehring, W.J. (1987) Expression of the *caudal* gene in the germ line of *Drosophila*: formation of an RNA and protein gradient during early embryogenesis. *Cell* **48**: 465–478.

Mlodzik, M., Fjose, A. and Gehring, W.J. (1985) Isolation of *caudal*, a *Drosophila* homeo box-containing gene with maternal expression, whose transcripts form a concentration gradient at the pre-blastoderm stage. *EMBO J* **4**: 2961–2969.

Nakabachi, A., Shigenobu, S., Sakazume, N., Shiraki, T., Hayashizaki, Y., Carninci, P. *et al*. (2005) Transcriptome analysis of the aphid bacteriocyte, the symbiotic host cell that harbors an endocellular mutualistic bacterium, *Buchnera*. *Proc Natl Acad Sci U S A* **102**: 5477–5482.

Nakamura, T., Yoshizaki, M., Ogawa, S., Okamoto, H., Shinmyo, Y., Bando, T. *et al*. (2010) Imaging of transgenic cricket embryos reveals cell movements consistent with a syncytial patterning mechanism. *Curr Biol* **20**: 1641–1647.

Nakao, H. (2012) Anterior and posterior centers jointly regulate *Bombyx* embryo body segmentation. *Dev Biol* **371**: 293–301.

Olesnicky, E.C. and Desplan, C. (2007) Distinct mechanisms for mRNA localization during embryonic axis specification in the wasp *Nasonia*. *Dev Biol* **306**: 134–142.

Olesnicky, E.C., Brent, A.E., Tonnes, L., Walker, M., Pultz, M.A., Leaf, D. *et al*. (2006) A *caudal* mRNA gradient controls posterior development in the wasp *Nasonia*. *Development* **133**: 3973–3982.

Peel, A.D., Chipman, A.D. and Akam, M. (2005) Arthropod segmentation: beyond the *Drosophila* paradigm. *Nat Rev Genet* **6**: 905–916.

Pellettieri, J. and Seydoux, G. (2002) Anterior-posterior polarity in *C. elegans* and *Drosophila* – PARallels and differences. *Science* **298**: 1946–1950.

Schmitt-Engel, C., Cerny, A.C. and Schoppmeier, M. (2012) A dual role for *nanos* and *pumilio* in anterior and posterior blastodermal patterning of the short-germ beetle *Tribolium castaneum*. *Dev Biol* **364**: 224–235.

Schoppmeier, M., Fischer, S., Schmitt-Engel, C., Lohr, U. and Klingler, M. (2009) An ancient anterior patterning system promotes *caudal* repression and head formation in ecdysozoa. *Curr Biol* **19**: 1811–1815.

Schröder, R. (2003) The genes *orthodenticle* and *hunchback* substitute for bicoid in the beetle *Tribolium*. *Nature* **422**: 621–625.

Schröder, R., Beermann, A., Wittkopp, N. and Lutz, R. (2008) From development to biodiversity – *Tribolium castaneum*, an insect model organism for short germband development. *Dev Genes Evol* **218**: 119–126.

Schulz, C. and Tautz, D. (1995) Zygotic *caudal* regulation by *hunchback* and its role in abdominal segment formation of the *Drosophila* embryo. *Development* **121**: 1023–1028.

Schulz, C., Schröder, R., Hausdorf, B., Wolff, C. and Tautz, D. (1998) A *caudal* homolog in the short germ band beetle *Tribolium* shows similarities to both, the *Drosophila* and the vertebrate *caudal* expression patterns. *Dev Genes Evol* **208**: 283–289.

Shigenobu, S., Bickel, R.D., Brisson, J.A., Butts, T., Chang, C-C., Christiaens, O. *et al*. (2010) Comprehensive survey of

developmental genes in the pea aphid, *Acyrthosiphon pisum*: frequent lineage-specific duplications and losses of developmental genes. *Insect Mol Biol* **19** (Suppl 2): 47–62.

Shinmyo, Y., Mito, T., Matsushita, T., Sarashina, I., Miyawaki, K., Ohuchi, H. *et al*. (2005) *caudal* is required for gnathal and thoracic patterning and for posterior elongation in the intermediate-germband cricket *Gryllus bimaculatus*. *Mech Dev* **122**: 231–239.

Stauber, M., Prell, A. and Schmidt-Ott, U. (2002) A single Hox3 gene with composite *bicoid* and *zerknüllt* expression characteristics in non-Cyclorrhaphan flies. *Proc Natl Acad Sci U S A* **99**: 274–279.

Stauber, M., Lemke, S. and Schmidt-Ott, U. (2008) Expression and regulation of *caudal* in the lower cyclorrhaphan fly *Megaselia*. *Dev Genes Evol* **218**: 81–87.

Takaoka, K. and Hamada, H. (2012) Cell fate decisions and axis determination in the early mouse embryo. *Development* **139**: 3–14.

The International Aphid Genomics Consortium (2010) Genome sequence of the pea aphid *Acyrthosiphon pisum*. *Plos Biol* **8**: e1000313.

Weaver, C. and Kimelman, D. (2004) Move it or lose it: axis specification in *Xenopus*. *Development* **131**: 3491–3499.

Will, L. (1888) Entwicklungsgeschichte der viviparen Aphiden. *Zool Jahrb Anat* **3**: 201–286.

Wilson, M.J., Havler, M. and Dearden, P.K. (2010) *Giant*, *Krüppel*, and *caudal* act as gap genes with extensive roles in patterning the honeybee embryo. *Dev Biol* **339**: 200–211.

Wolff, C., Sommer, R., Schröder, R., Glaser, G. and Tautz, D. (1995) Conserved and divergent expression aspects of the *Drosophila* segmentation gene *hunchback* in the short germ band embryo of the flour beetle *Tribolium*. *Development* **121**: 4227–4236.

Xu, X., Xu, P.X. and Suzuki, Y. (1994) A maternal homeobox gene, *Bombyx caudal*, forms both mRNA and protein concentration gradients spanning anteroposterior axis during gastrulation. *Development* **120**: 277–285.

Supporting Information

Additional Supporting Information may be found in the online version of this article at the publisher's web-site:

Figure S1. Developmental expression of ApHb protein during oogenesis and early embryogenesis in the asexual pea aphid. Germaria and anterior region of egg chambers are to the left. Immunostaining protocols were as described by Chang *et al*. (2006). (A) Ovarioles stained with affinity-purified antibody against ApHb protein. Staining signals of ApHb were identified in germaria and cytoplasm of embryos undergoing nuclear division (here we present staining results in stage-3 embryos as an example). Intensity of ApHb signals declined in embryos undergoing blastulation (stages 5–6 of development). Arrowhead and hollow arrowhead indicate places where localization of *Aphb* mRNA was shown in stage-3 and stage-6 embryos in Fig. 5A, respectively. (B) Negative control. Ovarioles were stained without the application of primary antibody. No staining signals were detected. For abbreviations please refer the legend of Fig. 2. Scale bar, 20 μm.